The Rotor-Oscillator Flow: Searching for Coherence amidst Chaos

By

Sarah Fay

Submitted to the
Department of Mechanical Engineering
in Partial Fulfillment of the Requirements for the Degree of

Bachelor of Science in Mechanical Engineering

at the

Massachusetts Institute of Technology

June 2015

Signature of Author: Signature redacted
Department of Mechanical Engineering
May 7, 2015

Certified by: Signature redacted
Thomas Peacock
Associate Professor of Mechanical Engineering
Thesis Supervisor

Accepted by: Signature redacted
Anette Hosoi
Professor of Mechanical Engineering
Undergraduate Officer

The Rotor-Oscillator Flow: Searching for Coherence amidst Chaos

by

Sarah Fay

Submitted to the Department of Mechanical Engineering
on May 7, 2015 in Partial Fulfillment of the
Requirements for the Degree of

Bachelor of Science in Mechanical Engineering

ABSTRACT

Chaotic mixing of highly viscous fluids is common in many biological and industrial processes. This study aims to gain insight about the properties of such common processes by examining one particular case of viscous, chaotic mixing: the rotor-oscillator flow. For some couplings of the rotor motion with its oscillation, this flow has been shown to have coherent islands of fluid parcels surrounded by a sea of chaos. Through finite-time Lyapunov exponent (FTLE) analysis, a roughly optimal coupling was found. The parameters that describe this coupling are the nondimensional oscillation amplitude $\varepsilon = 0.125$ and frequency $\lambda = 0.4\pi$. In order to understand more about the mixing of slow-moving, highly viscous fluids, these values can and will be explored experimentally and through braid theory to further examine the regions of coherence in this generally chaotic flow.

Thesis Supervisor: Thomas Peacock
Title: Associate Professor of Mechanical Engineering

Acknowledgements

I would like to thank Professor Peacock for taking me on as an undergraduate thesis student and providing me with the guidance and resources to work on such an interesting project. I would also like to thank Margaux Filippi for her constant support and enthusiasm for the work we did together. Matthieu Leclair is the numerical superstar who provided the MATLAB code and technical support for this project. Finally, I would like to thank my family and my housemates for encouraging me and inspiring my dedication to this work.

Table of Contents

List of Figures

List of Tables

1. Introduction

Many biological and industrial processes rely on the effective mixing of slow-moving, highly viscous fluids.[1] In order to improve upon these existing processes and perhaps engineer new mixing devices, a more comprehensive understanding of high viscosity chaotic flows needs to be attained. The study of such flows begins by exploring mixing environments that can be described completely analytically. The rotor-oscillator flow is one particular example of a mixing pattern whose governing equations have been derived and can be easily tested experimentally. The flow, as it is explored in this study, is generated by a long, slender rotor that rotates with a constant angular velocity and oscillates longitudinally within a wave tank. The experimental set-up for this flow is shown in Figure 1.

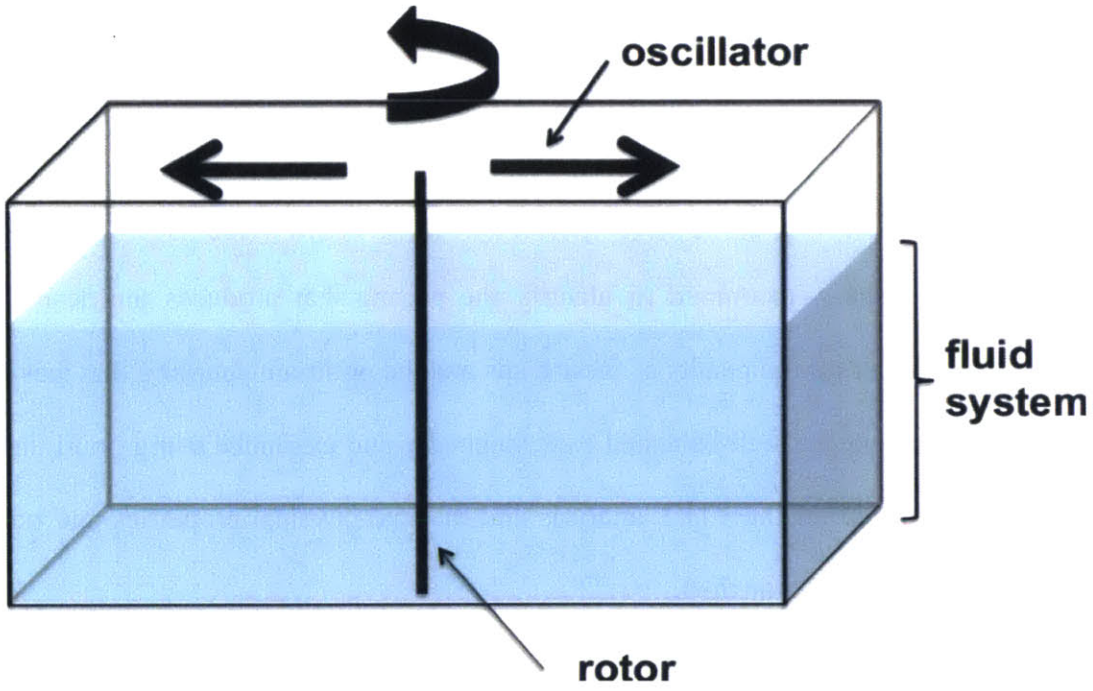

Figure 1: Diagram of the rotor-oscillator flow. The slender rotor spins with constant angular velocity and oscillates longitudinally within the tank.[2]

Hackborn, Ulucakli & Yuster were the first to explore the rotor-oscillator flow, but their work focuses on a slightly different version of the flow than is used in this study.[1] However, from these equations, Weldon et al.[3] went on to determine the analytical solution for the rotor-oscillator situation depicted in Figure 1. Both the Hackborn et al. study and later work that focuses on braid theory by Filippi[2] revealed that certain couplings of the rotor angular speed with its oscillation created an interesting flow environment that was dominated by chaotic mixing but contained some islands of coherence. These islands are common of highly viscous chaotic flows and are defined by Kaper & Wiggins to be regions in a flow where particles cannot enter or leave.[4] Islands are common to highly viscous chaotic flows.[4] The results of these previous works are presented in Section 2 of this study. This unique flow with coherent islands surrounded by a sea of chaos may be both analogous to observed viscous flows and a valuable source of inspiration for future mixing devices.

This study focuses on the use of finite-time Lyapunov exponents (FTLE) in distinguishing between chaotic regions of the flow and coherent ones. This analytical method is outlined in Section 3. For many different couplings of the rotor speed with its oscillatory motion, FTLE fields were generated and visually examined to identify the pairing that produces the desired flow behavior. Section 4 discusses the results of these trials and the optimum coupling that was found. In the future, these parameters will be tested experimentally and examined using braid theory to determine both the success of the FTLE analysis and the true physical properties and potential applications of the rotor-oscillator flow.

2. The rotor-oscillator flow

The flow examined in this study is called the rotor-oscillator flow. It was first characterized both theoretically and experimentally by Hackborn et al. This flow is generated in an incompressible fluid by two moving elements: a rotor and an oscillator. It is a two-dimensional Stokes flow, meaning it is dominated by viscous rather than inertial forces. The authors derived the governing equations of the flow field under these assumptions and ran physical experiments to confirm the success of their theoretical work. While their efforts are the basis for the numerical work in this study, we use a slightly modified version of their equations, originally derived by Weldon et al. to reflect the experimental setup depicted in Figure 1. The results of these studies are the motivation for the parameter exploration in this work.

2.1 The Hackborn, Ulucakli & Yuster analytical solution

In the flow explored by Hackborn et al., the rotor is a cylinder of radius a rotating at an angular speed ω. This rotor lies at a position $(c, 0)$ between two infinite parallel plates occupying $x = h$ and $x = -h$, and it extends infinitely in the z-direction. The oscillator is the plate at $x = h$; it translates in the y direction with velocity given by $V\cos(\alpha t)$. The stream function of this flow is ψ. Using the following nondimensionalization:

$$\frac{x}{h} \to x, \qquad \frac{y}{h} \to y, \qquad \frac{c}{h} \to c, \qquad \frac{\psi}{a^2\omega} \to \psi, \qquad \frac{ta^2\omega}{h^2} \to t, \tag{1}$$

and under the assumptions that the flow is in fact a Stokes flow and that the radius of the rotor is zero, the authors determined the governing equations to be

$$\frac{dx}{dt} = -\frac{\partial\psi}{\partial y}, \qquad \frac{dy}{dt} = \frac{\partial\psi}{\partial x} + \varepsilon(1 + x)\cos(\lambda t). \tag{2}$$

They define this nondimensional stream function to be

$$\psi = \frac{1}{2}\log[F(x,y)] + \int_0^\infty G(x,k)\cos(ky)\,dk, \tag{3}$$

with

$$F(x,y) = \frac{1 - 2e^{\pi y/2}\cos\left[\frac{1}{2}\pi(x-c)\right] + e^{\pi y}}{1 + 2e^{\pi y/2}\cos\left[\frac{1}{2}\pi(x+c)\right] + e^{\pi y}} \tag{4}$$

and

$$\begin{aligned} G(x,k) = &\frac{2[\tanh(k)\cosh(kx) - x\sinh(kx)]\cosh(kc)}{\sinh(2k) + 2k} \\ &+ \frac{2[\coth(k)\sinh(kx) - x\cosh(kx)]\sinh(kc)}{\sinh(2k) - 2k}. \end{aligned} \tag{5}$$

In these nondimensional governing equations, there are three important parameters: c, λ, and ε. The parameter, c, is simply the nondimensionalized position of the rotor. λ is the nondimensional frequency of the oscillation of the plate. ε is the nondimensional velocity amplitude of velocity of this oscillation, which is directly proportional to the displacement amplitude by a factor of λ. These two parameters are given by

$$\lambda = \frac{h^2\alpha}{a^2\omega} \tag{6}$$

and

$$\varepsilon = \frac{Vh}{2a^2\omega}. \tag{7}$$

The work of Hackborn et al. focuses on the impact of these two parameters on the behavior of the rotor-oscillator flow.

2.2 Experimental flow considerations

The theoretical analysis of the rotor-oscillator flow relies on four important assumptions that Hackborn et al. needed to account for and test in their physical experiments. The first assumption is that the flow must be a Stokes flow, meaning the Reynolds number, Re, must be much less than one. In this particular flow, the authors define this flow parameter to be

$$Re = \frac{a^2\omega}{\nu} \tag{8}$$

where ν is the kinematic viscosity of the fluid. For a given selection of λ and ε, the rotor angular velocity, ω, and the true frequency and amplitude of oscillation, α and V/α respectively (or V for the velocity amplitude of oscillation) are constrained by the assumption of Stokes flow. The experimental apparatus is limited in its range of executable ω, α, and V, and thus some selections of λ and ε, will not be experimentally feasible.

The second assumption is that the radius of the rotor is zero. Hackborn et al. found that the non-zero radius, a, of the real rotor did cause a significant difference between the theoretical and experimental flows for a given parameter set. This effect was amplified for larger rotor radii. They found, however, that even though the two flows were different, the theoretical flow generated for the nondimensional parameter $c = 0.54$ was nearly the same as the experimental flow generated for $c = 0.49$. By making this correction ($c = 0.54$) in their theoretical trials, they were able to reliably explore the parameter space computationally before testing experimentally.

The third assumption is that the plates are infinite. The end walls of the wave tank naturally limit the reality of this assumption, but Hackborn et al. found that their setup with wall ratio 4:1 did not create a flow significantly different from the theoretical flow with infinitely long walls. The reality of the fourth and final assumption (that the flow continues infinitely in the z direction) is also limited by the wave tank. In the theoretical flow, the potential effects of having a top and

bottom fluid surface (constraining the flow in the z direction) were not accounted for. The authors found, however, that these physical limitations did not cause significant differences between the experimental and theoretical flows.

2.3 The modified rotor-oscillator flow

Our study focuses on an adaption of the rotor-oscillator flow that was original studied by Weldon et al. The adaptation accounts for the difference between the Hackborn et al. experimental apparatus and the apparatus that will be used to experimentally test the results of this study. The primary difference between the two is that in this study, the oscillator is no longer the plate at $x = h$; it is the rotor, now translating with velocity $V\cos(\alpha t)$ while still continuing to rotate at angular speed ω. The governing equations[3] that reflect this physical difference are

$$\frac{dx}{dt} = -\frac{\partial\psi(x,\ y+\varepsilon\sin(\lambda t))}{\partial y}, \qquad \frac{dy}{dt} = \frac{\partial\psi(x,\ y+\varepsilon\sin(\lambda t))}{\partial x} \tag{9}$$

where the nondimensional stream function, velocity amplitude of the oscillation, and oscillation frequency (ψ, ε, and λ respectively) are still defined by Equations (3)-(7).

These governing equations are natural based on the same four assumptions that Hackborn et al. made, and we need to take similar care in testing and accounting for any differences these might cause in the future experimental trials of this study. First, our physical flow must also meet the criteria $Re << 1$. This flow number is still given by Equation (8), but in our case, h will reflect the dimensions of our own wave tank. Given the capabilities of our experimental system (limitations on the setting of rotor angular velocity, frequency of oscillations, and amplitude of oscillations), we will also be constrained in the range of parameter values (λ and ε) we will be able to experimentally observe. Like Hackborn et al., any result we find in our theoretical trials must satisfy these criteria or else we will not be able to support it with experimental data.

Filippi's work was performed on the experimental apparatus this study's results will be tested on. Her work showed that the same correction ($c = 0.54$) should be made to the theoretical trials to be able to accurately represent the experimental flow that will result in the tank with $c = 0.49$. Our study therefore uses $c = 0.54$ in all numerical trials, to ensure that the results will reflect the physical flow when it is tested. Filippi also found that neither the finite dimensions of the rectangular tank (2.5:1) nor the top and bottom surfaces caused significant discord between her theoretical and experimental results. These findings suggest that our study can, in fact, be translated and tested in the experimental system available to us.

2.4 Historical results

In their work, Hackborn et al. studied the rotor-oscillator flow using Poincaré maps and found that there were some parameter values for which the resulting flow was generally chaotic with islands of coherence; this was not the objective of their work and thus was not explored further in their study. Filippi discovered this same result and found, using braid theory, that a sparse number of particles could be used to identify this qualitative behavior. This study aims to use finite-time Lyapunov exponent (FTLE) fields to examine the rotor-oscillator flow with the intention of identifying a parameter set for which the flow exhibits clear islands of coherence surrounded by a sea of chaos.

3. Finite-time Lyapunov exponents (FTLE)

Unlike the works of Filippi and Hackborn et al., this study focuses on the analysis of finite-time Lyapunov exponents (FTLE) fields to examine the rotor-oscillator flow. The FTLE of a given point in a flow is a single number indicating how sensitive the trajectory of a particle starting at

that point is to its initial conditions; it is thus a measure of how chaotic the flow is expected to be at that point.

In this study, the FTLE is calculated at a particular point (x,y) in a flow by numerically advecting four particles from positions[5] A_0: $(x+\Delta x/2, y)$, B_0: $(x-\Delta x/2, y)$, C_0: $(x, y+\Delta y/2)$, and D_0: $(x, y-\Delta y/2)$. In these numerical trials, Δx and Δy are taken to be 10^{-5}. The particles were advected over a time window, Δt, using Equation (9) and the Runge-Kutta method with time step 0.1. Given Equation (9)'s dependence of the parameters λ and ε, the positions A_f, B_f, C_f, and D_f of the particles after advection will also depend on these parameters. From these final particle positions, the gradient of the flow map at the original point, $\nabla \boldsymbol{F}_{\Delta t}(x, y)$, is calculated by this relation: [5]

$$\nabla \boldsymbol{F}_{\Delta t}(x,y) = \begin{bmatrix} \dfrac{x_{A_f} - x_{B_f}}{\Delta x} & \dfrac{x_{C_f} - x_{D_f}}{\Delta y} \\ \dfrac{y_{A_f} - y_{B_f}}{\Delta x} & \dfrac{y_{C_f} - y_{D_f}}{\Delta y} \end{bmatrix}. \tag{10}$$

This gradient is itself a measure of how much the particle trajectory from (x, y) is influenced by small displacements, but it is not yet a good measure of chaos given its matrix format and its basis in the Cartesian frame.[4] The next step towards calculating the FTLE is to compute the right Cauchy-Green strain tensor, $\boldsymbol{C}_{\Delta t}(x, y)$, by the following relation:[5]

$$\boldsymbol{C}_{\Delta t} = \nabla \boldsymbol{F}^T \nabla \boldsymbol{F} \tag{11}$$

This strain tensor provides a new measure of chaos that is no longer rooted in the Cartesian frame, and its largest eigenvalue, λ_2 (where $0 \leq \lambda_1 \leq \lambda_2$), measures the magnitude of the maximum divergence of two particles in the flow starting near point (x, y) over the time window Δt. Note that λ_1 and λ_2 are eigenvalues of the Cauchy-Green strain tensor, whereas λ is the nondimensional frequency of oscillation in the flow. The finite-time Lyapunov exponent (FTLE) for the time window Δt is then computed as follows:[5]

$$FTLE = \frac{1}{2\Delta t}\log(\lambda_2). \tag{12}$$

The FTLE represents how divergent the flow field is at (x, y). Higher FTLE values represent higher sensitivity to initial conditions, and likely more chaotic flow.

In this study, FTLEs are calculated for 100,000 points on a grid of positions in the relevant domain of the rotor-oscillator flow that is realizable with the available experimental system (x ranging from -1 to 1 and y ranging from -2.5 to 2.5). The FTLEs are then mapped to a color gradient and plotted by their position in the domain. Given the dependence of the FTLE value on Δt, the maximum FTLE and thus the color scale are also primarily dictated by the time window selected for the trial. Figure 2 shows an example of an FTLE map created in this study for the rotor-oscillator flow when $\varepsilon = 0$, meaning it is steady with no oscillatory motion.

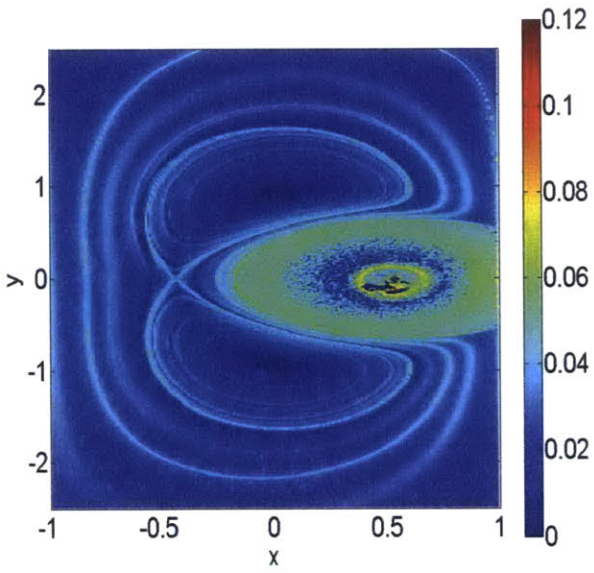

Figure 2: A steady flow FTLE field. The color map of the FTLE values for the rotor-oscillator flow when $\varepsilon = 0$ taken over a 120 unit time window.

The warmer colors represent areas of higher FTLE, more chaotic regions, while the cooler colors represent areas of lower FTLE, less chaotic, more coherent regions. This steady case has two areas of very low FTLE that seem to constitute coherent islands, in what resemble two butterfly wings

centered near (0, -1) and (0, 1). These wings are surrounded by areas of generally low FTLE values. By generating FTLE maps for different parameter sets, this study aims to detect these coherent islands, regions of low FTLE, but islands that are surrounded by a chaotic sea, high FTLE values that fill the nearby domain. FTLE maps are an easily digested, visual tool that will allow the desired flow behavior to be identified.

4. Results

In this study, FTLE fields were generated for nondimensional frequencies, λ, ranging from $\pi/60$ to 4π and velocity amplitudes of oscillation, ε, from 0.005 to 1. FTLE values were calculated for a grid of particles of resolution 0.01 for the relevant domain of the flow (x ranging from -1 to 1 and y ranging from -2.5 to 2.5). Trials were performed for several different time windows, but much of the comparisons were performed for FTLE fields calculated over a 120 unit time window. Of the different parameter sets that were tested, the FTLE field for $\lambda = 0.4\pi$ and $\varepsilon = 0.125$ had the clearest coherent islands that were nested in a generally chaotic flow.

4.1 Trials with varying frequency of oscillation

With $\varepsilon = 0.125$, FTLE fields were generated for ten different nondimensional frequencies of the oscillation, λ, ranging from $\pi/60$ to 4π. Small frequencies on the order of 0.1 and large frequencies on the order of 10 both seemed to exhibit coherent behavior similar to the steady flow case shown in Figure 2. At intermediate frequencies on the order of 1, the flow appeared to be overall chaotic. In the transition from intermediate and large values of the nondimensional frequency, an FTLE field was observed that matched the desired characteristics, regions of low FTLE surrounded by overall high FTLE regions.

For small values of λ on the order of 0.1, the rotor-oscillator FTLE field resembles that of the steady state flow (where ε is 0). Figure 3 compares the FTLE field for λ equal to (a) $\pi/30$ and (b) $\pi/60$ for a 120 unit time window. The steady flow case is presented in Figure 2.

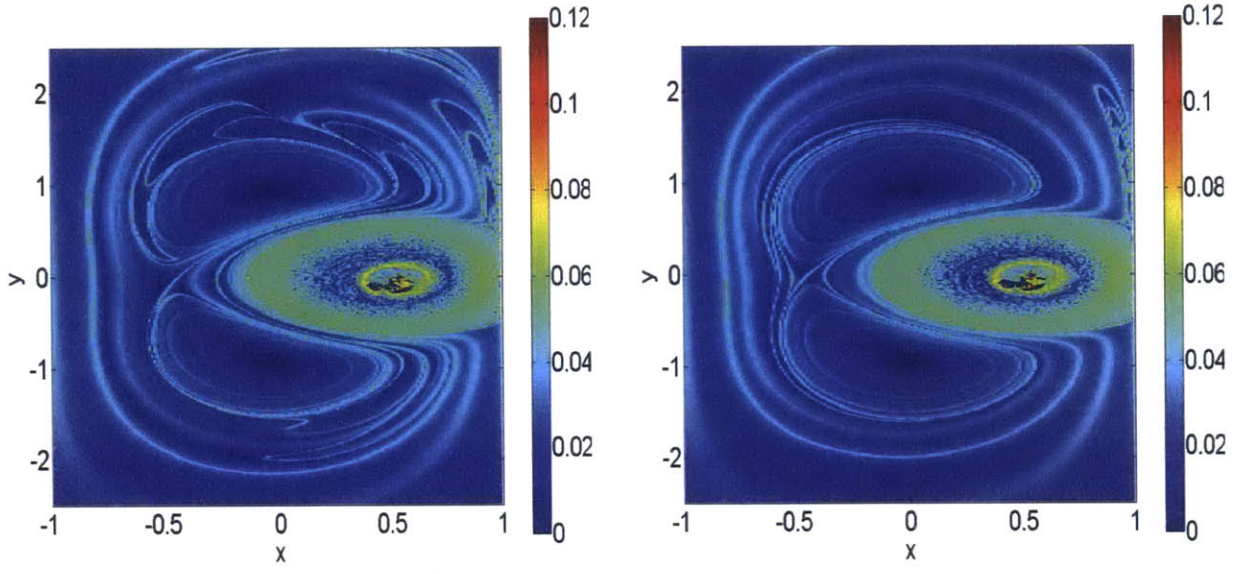

Figure 3: FTLE fields for small λ. The color maps of the FTLE values for the rotor-oscillator flow with $\varepsilon = 0.125$ over a 120 unit time window. The frequencies of oscillation are (a) $\lambda = \pi/30$ (~0.10) and (b) $\lambda = \pi/60$ (~0.05).

All three of these FTLE fields are populated with areas of low FTLE outside of the region surrounding the rotor centered at (0.54, 0). This suggests that the flow is generally coherent rather than chaotic. Like the steady flow, there appear to be coherent islands that make up the two butterfly wings again centered near (0, -1) and (0, 1), but still, they are not surrounded by a sea of chaos. The flow with slower oscillations, λ equal to $\pi/60$, has clearer regions of low FTLE and more closely resembles that of the steady flow. This result is expected because slowing down the oscillations infinitely should essentially produce the steady state flow.

For large values of λ on the order of 10, the rotor-oscillator flow also exhibits ordered flow that has qualitative similarities to the steady state flow. Figure 4 shows the FTLE field for λ equal to (a) 2π and (b) 4π. Recall again that the steady state flow is depicted in Figure 2.

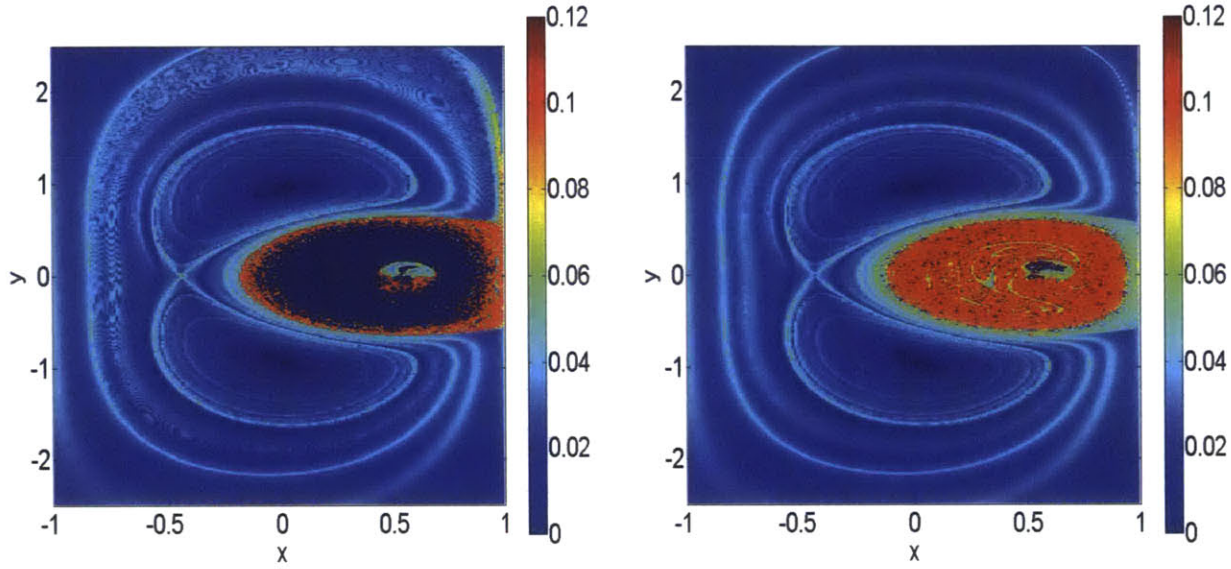

Figure 4: FTLE fields for large λ. The color maps of the FTLE values for the rotor-oscillator flow with $\varepsilon = 0.125$ over a 120 unit time window. The frequencies of oscillation are (a) $\lambda = 2\pi$ (~6.28) and (b) $\lambda = 4\pi$ (~12.57).

Like in the low frequency and steady state cases, the two butterfly wings appear near (0, -1) and (0, 1). Similarly, outside of the flow near the rotor, the FTLE field is all low valued, meaning the flow is generally coherent. The difference between these FTLE fields and those of small λ is primarily evident in the flow near the rotor. For $\lambda = 4\pi$, this area is much more chaotic than it was in the (near) steady state cases. However, for $\lambda = 2\pi$, the area near the rotor is mostly composed of low (near zero) FTLE values.

We do not believe this reflects the true behavior of the flow for these parameters but is instead an artifact of the time-step used to approximate the particle trajectories through the Runge-Kutta method. The error of this approximation method is larger for larger time steps and for faster moving regions of the flow. This hypothesis was tested by generating the FTLE field for these

same parameters but with a time-step of 0.01 rather than 0.1. The result of this trial is shown in Figure 5.

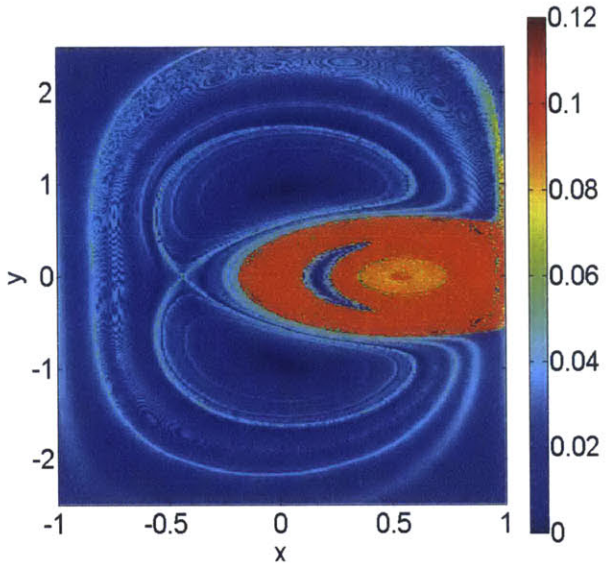

Figure 5: An FTLE field for $\lambda = 2\pi$ with R-K time step = 0.01. The color map of the FTLE values for the rotor-oscillator flow with $\varepsilon = 0.125$ and $\lambda = 2\pi$ over a 120 unit time window but using 0.01 as the Runge-Kutta time step rather than 0.1.

These improved FTLE calculations suggest that near the rotor there is a more uniform, relatively chaotic flow rather than a completely coherent region. Note, however, that there remains an interesting crescent moon shaped region of low FTLE contained in this area, which may or may not also be a result of approximation error. This trial is a reminder that the Runge-Kutta time-step can serve an important role and needs to be considered when conclusions are drawn from the generated FTLE fields.

A "sea" of chaos only seemed to appear at intermediate frequencies of oscillation, those of order 1. Figure 6 shows the FTLE field for λ equal to 0.2π.

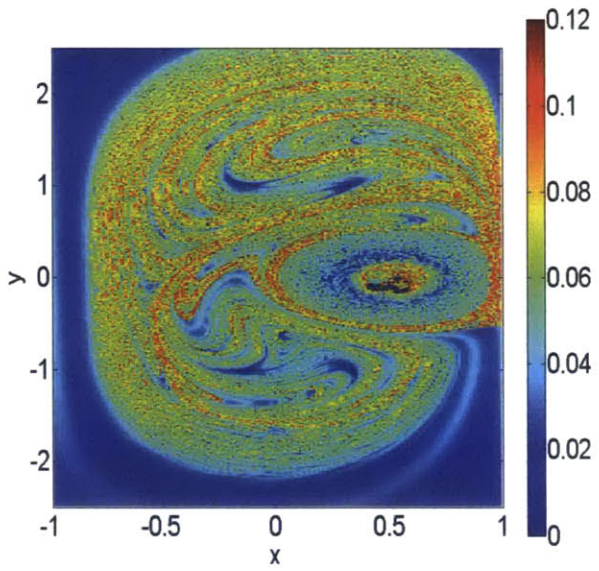

Figure 6: An FTLE field for intermediate λ. The color map of the FTLE values for the rotor-oscillator flow with $\varepsilon = 0.125$ and $\lambda = 0.2\pi$ over a 120 unit time window.

This flow has consistently high FTLE values engulfing the entire region of active flow, including the region where previous trials have shown clear butterfly wings. The flow appears to be generally chaotic, but the coherent islands are no longer prominent.

These results suggest that the flow transitions from being generally coherent at low frequencies, to being generally chaotic at intermediate frequencies, and back to being coherent at high frequencies. This study aimed to identify a value of λ for which the flow exhibits regions of coherence, like the butterfly wings in Figure 2, surrounded by a large chaotic region like that seen at the intermediate λ equal to 0.2π in Figure 6. This study examined FTLE fields for frequency values in these two transition regions (low to intermediate values and intermediate to high values). The FTLE field for λ equal to 0.4π was generated and is shown in Figure 7.

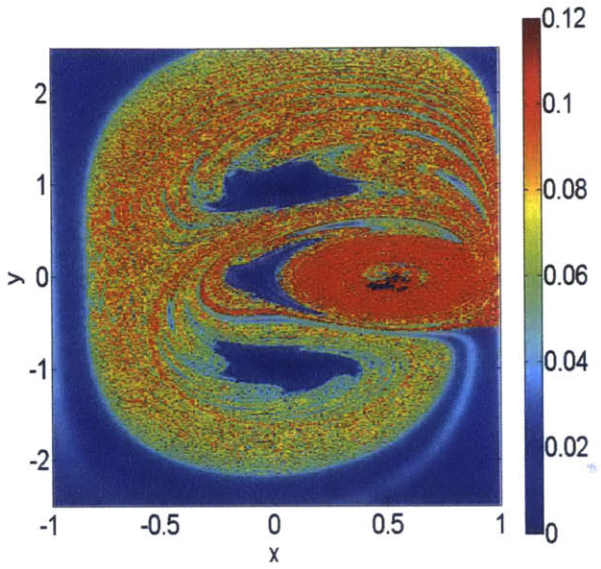

Figure 7: An FTLE field for $\lambda = 0.4\pi$. The color map of the FTLE values for the rotor-oscillator flow with $\varepsilon = 0.125$ and $\lambda = 0.4\pi$ over a 120 unit time window.

This FTLE field falls in the frequency transition from intermediate to high values, and it does show regions of coherence among regions of completely chaotic mixing. In addition to the butterfly wing areas of coherence observed in previous trials, this field shows a region of low FTLE centered near (0, 0). The presence of this third coherent island makes this parameter set particularly unique; this nondimensional frequency value, $\lambda = 0.4\pi$, shows the qualitative pattern desired in this study.

4.2 Trials with varying amplitude of oscillation

In order to further explore the parameter space, trials were run for each of these ten frequencies where FTLE fields were generated for eight nondimensional velocity amplitudes of oscillation, ε, ranging from 0.005 to 1. In general, the smallest amplitude values lead to near steady state flows, as may be expected given the rotor is almost stationary for ε near zero. The largest amplitude values lead to combinations of coherent and chaotic regions that are not easily distinguished and defined. This section will discuss only the effects of changing amplitude on the

FTLE fields at the frequency of interest, λ is 0.4π, even though the other frequencies were also examined.

Figure 8 shows FTLE fields for two representative values of ε: one low ($\varepsilon = 0.01$) and one high ($\varepsilon = 1$). A third intermediate value of ε (= 0.125) is presented in Figure 7.

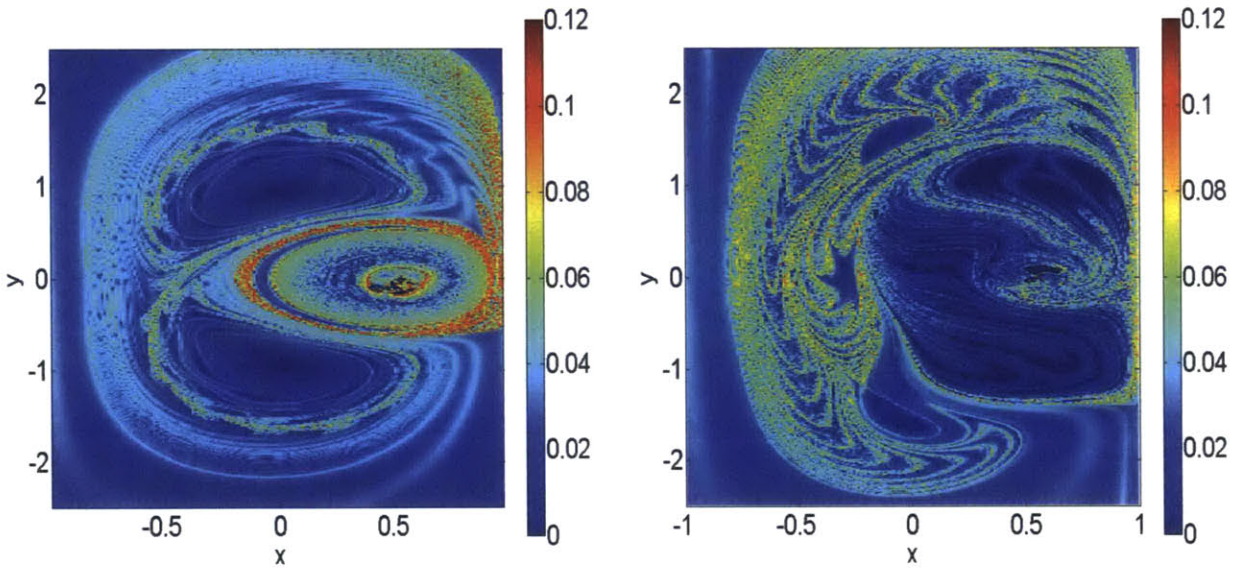

(a) (b)

Figure 8: FTLE fields for varying ε. The color maps of the FTLE values for the rotor-oscillator flow with $\lambda = 0.4\pi$ over a 120 unit time window. The velocity amplitudes of oscillation are (a) $\varepsilon = 0.01$ and (b) $\varepsilon = 1$.

As expected, the lowest amplitude flow depicted in Figure 8 (a), on the order of ε equal to 0.01, shows the familiar, relatively coherent flow characteristic of the steady flow. It does appear more chaotic than the steady flow chaos, but it has lost the most of the chaotic sea this study aims to detect. The largest amplitude flow depicted in Figure 8 (b), on the order of ε equal to 1, has many regions of high and low FTLE near each other. Defined regions and shapes of coherence are not easily identifiable in this case. The FTLE field for ε equal to 0.125 (order 0.1) better exhibits the desired flow characteristics than low or high valued amplitudes and in fact, with $\lambda = 0.4\pi$, is the parameter pair that best showed coherent islands surrounded by a generally chaotic flow.

4.3 Further trials with optimum parameters

Finally, to further justify the selection $\varepsilon = 0.125$ and $\lambda = 0.4\pi$, a trial was run over a 500 unit time window. The resulting FTLE field is shown in Figure 9.

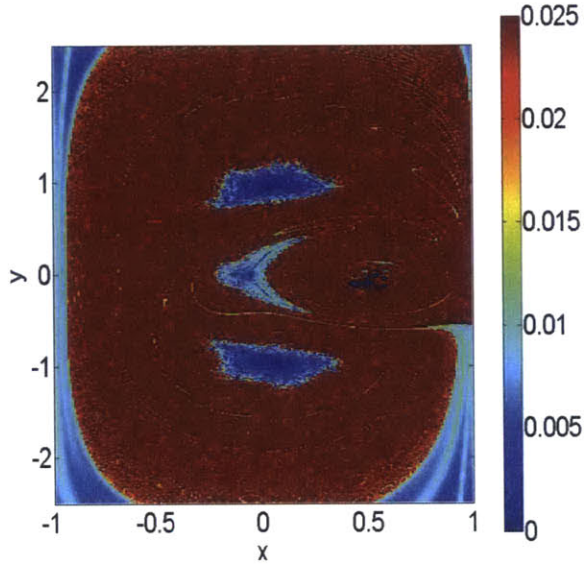

Figure 9: Trial of optimal parameters for a long time window. The color map of FTLE values for the rotor-oscillator flow with $\varepsilon = 0.125$ and $\lambda = 0.4\pi$ over a 500 unit time window.

Even examining trajectories of particles over 100 periods of oscillation (calculating the FTLE for this time window) does not suggest that the particles in the islands begin to diverge significantly. The islands appear to be roughly the same size they were when the FTLE field was examined for the 120 unit time window (shown in Figure 7). The surrounding region, however, appears to become more uniformly chaotic. Important to note however, that all of these FTLE values are quite small compared to those observed in a smaller time window, a natural result given the dependence of the FTLE on Δt. Still, the overall result of this long time window trial supports the given parameter value selection in producing the desired flow behavior.

More importantly, however, trials were run using a reduced time step for the Runge-Kutta particle advections. Figure 10 (b) shows the result of a trial with time-step 0.01 for the selected

optimal parameters and a 120 unit time window. For direct comparison to the analogous trial with time-step 0.1, the FTLE field in Figure 7 is again presented in Figure 10 (a).

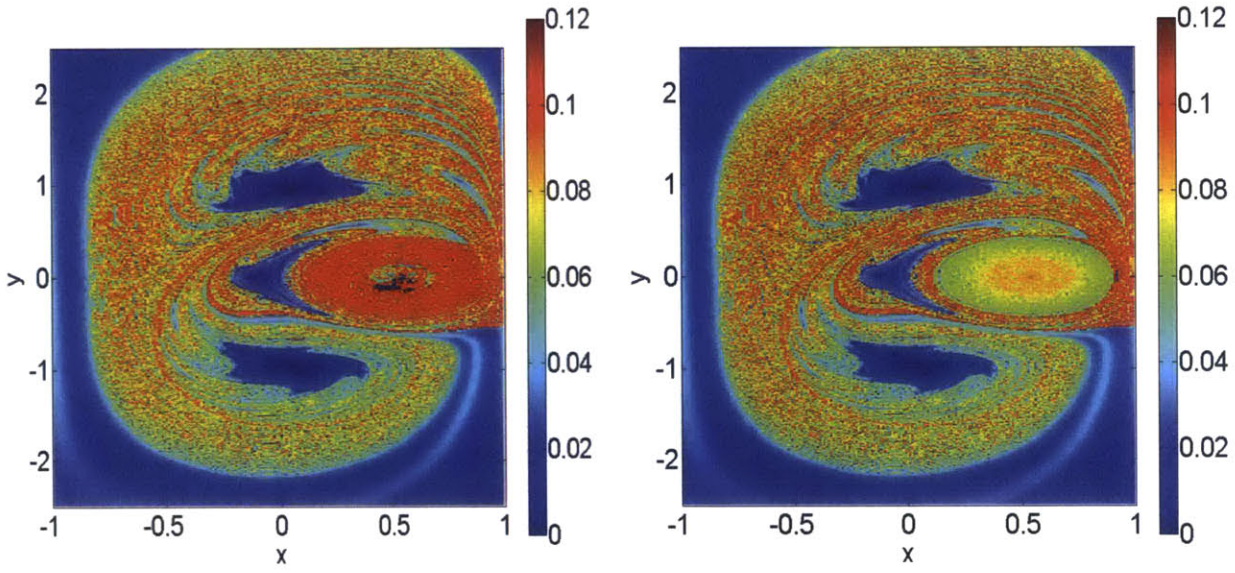

Figure 10: FTLE fields for optimal parameters with varying R-K time step. The color map of the FTLE values for the rotor-oscillator flow with $\varepsilon = 0.125$ and $\lambda = 0.4\pi$ over a 120 unit time window using (a) 0.1 and (b) 0.01 as the Runge-Kutta time step.

These two FTLE fields are qualitatively the same everywhere except in the region near the rotor. As with the trials in Figure 4 (a) and Figure 5, the smaller time-step appears to have reduced the error in particle trajectories in this region, producing an FTLE field that more closely resembles the coherent behavior expected near the rotor. The overall flow behavior, chaotic with coherent islands, is not notably changed by this improved FTLE analysis (by reducing the time-step by a factor of 10).

A trial was then performed with an even smaller Runge-Kutta time-step: 0.01. This FTLE field was only generated for a 60 unit time window in order reduce the computational resources required to perform such fine analysis. The resulting FTLE field is shown in Figure 11 (b), while the analogous one for a 60 unit time window and a time-step of 0.1 is shown in Figure 11 (a). Both trials were still run using $\varepsilon = 0.125$ and $\lambda = 0.4\pi$.

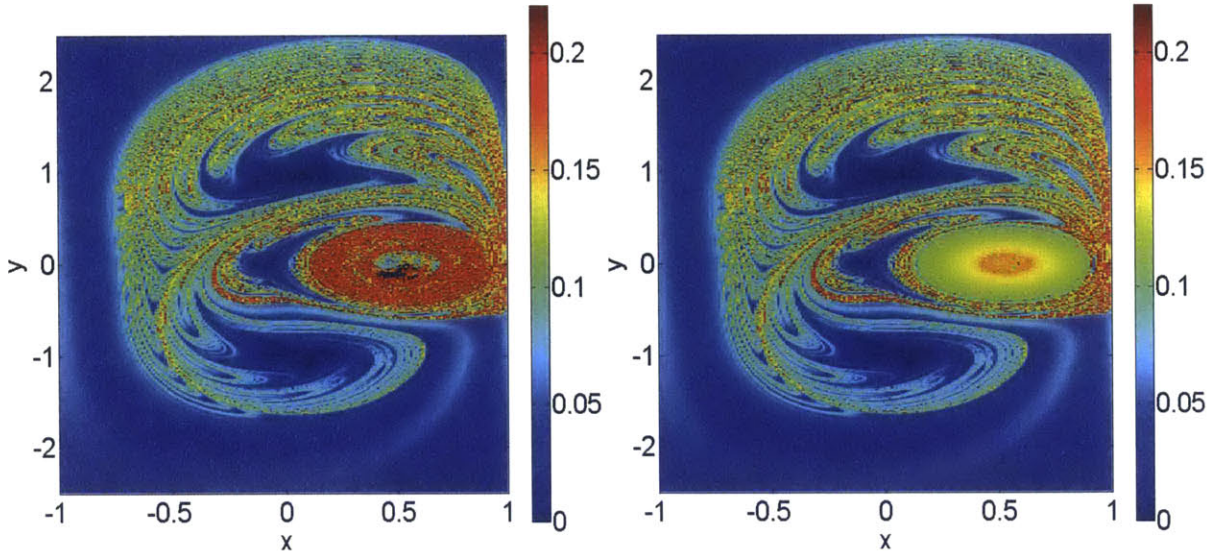

(a) (b)

Figure 11: A second trial using optimal parameters and varying R-K time step. The color map of the FTLE values for the rotor-oscillator flow with $\varepsilon = 0.125$ and $\lambda = 0.4\pi$ over a 60 unit time window using (a) 0.1 and (b) 0.001 as the Runge-Kutta time step.

Again, the two FTLE fields display the same qualitative behavior, including three coherent islands surrounded by a generally chaotic flow. The area near the rotor again appears to more closely resemble the expected behavior in this region for the trial with a finer time-step. Both of these reduced time-step trials support the selection of $\varepsilon = 0.125$ and $\lambda = 0.4\pi$ as optimal parameters for creating a generally chaotic flow that contains isolated coherent regions.

4.4 Comparison to historical data

The resulting parameter choices ($\varepsilon = 0.125$ and $\lambda = 0.4\pi$) of this exploratory study agree with Filippi's work on this same flow. Her work used Poincaré maps to identify the qualitative flow behavior this study aims to detect. She then employed braid theory to detect these regions from a sparse experimental data set. The rough results of that study propose that $\varepsilon = 0.125$ and $\lambda = 2.5$ (slightly more than 0.4π, or 1.26) give the same qualitative behavior that this study aims to detect. The result of the FTLE field generation for Filippi's parameters is depicted in Figure 12.

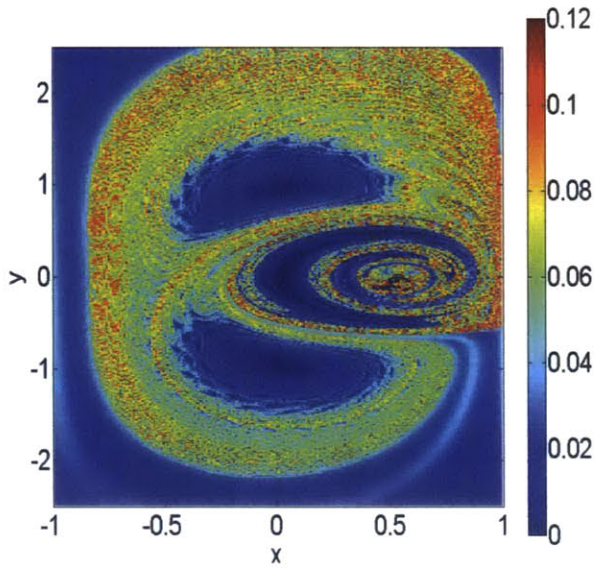

Figure 12: An FTLE field for the Filippi parameters. The color map of FTLE values for the rotor-oscillator flow with $\varepsilon = 0.125$ and $\lambda = 2.5$ over a 120 unit time window.

The result shows similar islands of coherence surrounded by chaos as this study's selected parameters (shown in Figure 7). However, this study's result shows an interesting third coherent island near (0, 0) and surrounding flow is more chaotic than in the Filippi case. The FTLE analysis performed in this study visually reveals the qualitative behavior of the rotor-oscillator flow and lead to the identification of parameter values ($\varepsilon = 0.125$ and $\lambda = 0.4\pi$) for a flow that contains coherent islands surrounded by a sea of chaos.

4.4 Experimental parameter equivalents

The identified nondimensional parameter values, $\varepsilon = 0.125$ and $\lambda = 0.4\pi$, correspond to physically feasible experimental parameters. The experimental apparatus that these results will be tested on has walls a distance, $2h$, of 0.1 m and a rotor radius, a, of 0.0015 m. From these physical values and a combination of the Equations (6) and (7), the displacement amplitude of oscillation, V/α, for these nondimensional parameters is computed to be approximately 0.0099 m, which falls within the dimensions of the apparatus.[6] An experimentally feasible angular velocity can then be

chosen, and using Equation (6), the frequency (and period) of oscillation, α (and T), can be computed. Table 1 shows these calculations for several feasible angular velocities, as well as the corresponding Reynolds numbers for flows with these parameters, where the kinematic viscosity is taken to be 1.36 Pa·s from the properties of the fluid previously used in the experimental apparatus by Filippi.

Table 1: Potential experimental parameters.[6] The experimental parameters (rotor angular velocity, ω, oscillation period, T, and Reynolds number, Re) that correspond to the nondimensional parameters $\varepsilon = 0.125$ and $\lambda = 0.4\pi$.

ω (RPM)	T (min:sec)	Re (rad)
200	4:25	0.045
600	1:28	0.135
800	1:06	0.180

These three potential angular velocities will produce a flow with a Reynolds number small enough for the experimental flow to feasibly match the theoretical flow.[5] Also, the corresponding oscillation frequencies, α, for these values of ω are feasible within the experimental parameters.

Setting the rotor velocity to be 200-800 rpm, the corresponding period of oscillation to be approximately between 1 and 4.5 minutes, and the displacement amplitude of oscillation to be 0.0099 m should yield an experimental flow that is generally chaotic with three islands of coherence.

5. Conclusions

For some values of the nondimensional parameters ε and λ, the rotor-oscillator flow field contains islands of coherence that are surrounded by a sea of chaotic mixing. Through the analysis of FTLE fields for different parameter sets, $\varepsilon = 0.125$ and $\lambda = 0.4\pi$ was the set that suggested the best realization of this particular flow behavior. λ was chosen to be 0.4π as it lies in the transition

from highly chaotic flow (observed at intermediate values of λ on the order 1) to highly coherent flow (observed at large values of λ on the order 10). ε was chosen to be 0.125 as it also lies in a transition from highly coherent flow at $\varepsilon = O(0.01)$ to highly chaotic flow at $\varepsilon = O(1)$. The analysis was performed for several different time windows and Runge-Kutta time-steps, and the results agree with the parameters Filippi had discovered in her work, which identified these regions using braid theory.

The most important next step in this study is testing these theoretical parameters with our experimental apparatus. The physical parameters that correspond to this λ and ε pair were computed and found to be feasible with the available experimental system. To execute this flow experimentally, the rotor velocity should be set in the 200-800 rpm range; the oscillation period should correspondingly be set in the 1-4.5 minute range; and the displacement amplitude of oscillation should be 0.0099 m. The theoretical rotor-oscillator flow for $\varepsilon = 0.125$ and $\lambda = 0.4\pi$ shows promise that the coming experimental trials and following braid theory analysis will in fact reveal a flow with coherent islands in a sea of chaotic mixing.

References

[1] Hackborn, W. W., Ulucakli, M. E., and Yuster, T., 1997, "A theoretical and experimental study of hyperbolic and degenerate mixing regions in a chaotic Stokes flow," J. Fluid Mech., 346, pp. 23-48.

[2] Filippi, M., 2015, "Untangling Tracer Trajectories and Clarifying Coherence Using Braid Theory," Ph. D. Qualifying Presentation, Massachusetts Institute of Technology, Cambridge, MA.

[3] Weldon, M., Peacock, T., Jacobs, G.B., Helu, M., and Haller, G., 2007, "Experimental and Numerical Investigation of the Kinematic Theory of Unsteady Separation," Under consideration for publication in J. Fluid Mech.

[4] Kaper, T. J., and Wiggins, S., 1993, "An analytical study of transport in Stokes flows exhibiting large-scale chaos in the eccentric journal bearing," J. Fluid Mech., 253, pp. 211-243.

[5] Peacock, T. and Allshouse, M.R., 2012, "A short course on Lagrangian Coherent Structures (LCSs) and their application to ocean surface transport," Course Notes, Massachusetts Institute of Technology, Cambridge, MA.

[6] Filippi, M., 2015, "Rotor-oscillator parameters," Notes for Master's Thesis, Massachusetts Institute of Technology, Cambridge, MA.